

# Transients Following the Energizing of High Voltage AC Cables with Shunt Compensation

S. Wijesinghe, K.K.M.A. Kariyawasam, B. Jayasekera, D. Muthumuni, M. Chowns

**Abstract--** This paper presents the challenges faced and the possible mitigation techniques when interconnecting an offshore wind power plant to the main grid through a shunt compensated AC cable(s). The AC cables form the onshore and offshore transmission system that connects the 1200 MW wind power plant to the 400 kV ac bus at the point of interconnection. Studies illustrate that static as well as dynamic shunt compensation is required to operate the overall system safely while meeting the specific grid code requirements of the system operator. Studies show that Zero missing phenomenon is one of the main concerns that must be addressed. This is observed when the cables are energized with the shunt reactors connected to the cable. One interesting observation is the impact of transformer saturation and the resulting waveform distortions. A literature review did not reveal any reporting of this observation. As such, this observation is further investigated and details are reported. Additionally, possible mitigation options such as distributing the reactors across different locations of the cable and the implementation of pre insertion breaker resistors are studied.

**Keywords:** Zero missing, offshore wind power plant, shunt compensation, HVAC cables.

## I. INTRODUCTION

OFFSHORE wind generation projects comprise of transmission systems capable of connecting the wind power plant to the closest onshore grid substation. Some of these projects utilize high voltage ac cables to transport the wind power to the onshore ac network. The ac cables under consideration for these projects include single core (coaxial) cables as well as three core (pipe type) cables.

Long ac cables present numerous technical challenges. The utilities must carefully evaluate the appropriate solutions and determine if the risks associated with implementing selected solution are acceptable.

AC cables consume significant amounts of capacitive reactive power. In order to reduce the burden on the interconnected ac system as well as on the wind generators, the cables should be compensated through the proper selection

of shunt reactive power compensation devices. This is essential to meet the transmission grid code requirements as well as to limit the temporary over voltage following the cable energization or system events such as load rejection.

The wind power plant under study is named Triton Knoll and is a 1.2 GW project to be installed by RWE Innogy. The wind power plant is located approximately 55 km off the North Norfolk coast on the North Sea. The interconnection point is located approximately 60 km inland from the coast line at the Bicker Fen 400 kV Sub- Station in East UK.

System design studies have indicated that a combination of FACTS based (STATCOM, SVC, etc.) shunts reactive power devices and shunt reactors gives the optimal reactive power compensation solution considering both technical and cost aspects.

Electromagnetic transient simulation studies on Triton Knoll offshore wind power plant were performed to investigate a number of technical concerns associated with energizing long ac cables with shunt reactors connected at the switching end. These include the transient over voltages upon cable energizing, cable charging current transients, discharge current transient during close by faults, transformer energizing and the 'zero missing' phenomenon.

Studies concluded that the main concern to be addressed is the 'zero missing' phenomenon. While 'zero missing' phenomenon is well understood, only a handful of past publications address the issue. This has been discussed and a theoretical explanation is presented in [1], [2]. In this paper, the relationship between the cable charging, the reactor size and the zero miss duration is analyzed in order to determine the acceptable risk. It should be noted that other breakers in the ac substation (and possibly elsewhere in the system) will also experience the 'zero miss' current, thereby making them vulnerable should they be required to interrupt a current during this period.

Another observation not previously reported is the current distortion following the closing of the breaker to energize the cable and the reactor. The observed current harmonics can be a power quality concern. EMT simulations and analysis are carried out to further investigate this observation. This is considered to be a new contribution of this paper. The paper concludes with suggested mitigation methods and remarks on acceptable risks.

## II. TRITON KNOLL OFFSHORE WIND POWER PLANT

Studies are carried out on the proposed 1.2 GW Triton Knoll wind power plant project. The overall project consists

---

S. Wijesinghe and M. Chowns are with RWE Innogy, Auckland House Lydiard Fields, Great Western Way, Swindon, SN5 8TZ, UK ([sarath.wijesinghe@rwe.com](mailto:sarath.wijesinghe@rwe.com), [mick.chowns@rwe.com](mailto:mick.chowns@rwe.com))

K. K. M. A. Kariyawasam, is with the Dept. of Electrical and Computer Eng., University of Manitoba, Canada ([umkapuge@cc.umanitoba.ca](mailto:umkapuge@cc.umanitoba.ca)).

D.Muthumuni and B.Jayasekera are with the Manitoba HVDC Research Centre, Canada ([dharsana@hvdc.ca](mailto:dharsana@hvdc.ca) , [Bathiya@hvdc.ca](mailto:Bathiya@hvdc.ca)).

of two phases, each being 600 MW. As shown in Fig. 1, onshore substation (400 kV- Bicker Fen Substation) is about 115 km away from the offshore wind power plant (marked in red).



Fig. 1 - Location of wind power plant [4]

The feasibility of using an AC transmission system (220 kV) to export power is investigated in this study. The proposed transmission configuration is illustrated in Fig. 2. A 54.4 km offshore cable (pipe type) and a 59.7 km onshore cable (coaxial) are used to interconnect the wind power plant to the grid. The total fixed shunt compensation required to support the AC transmission system while meeting grid code requirements was determined to be 270 MVar. This was determined based on steady state load flow analysis.

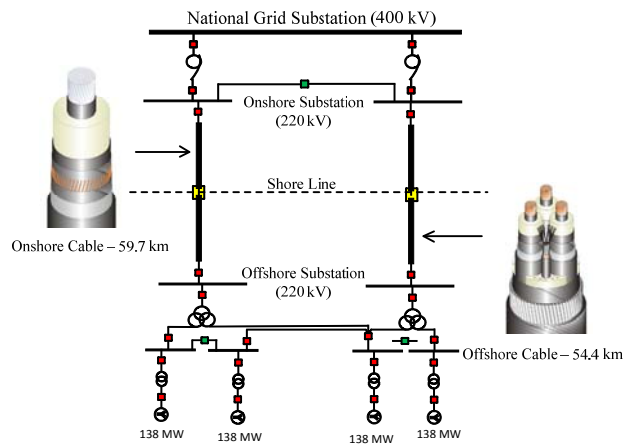


Fig. 2 – AC Transmission System Topology

### III. ZERO MISSING PHENOMENON

Wind power plant design studies concluded that the main concern to be addressed is the ‘zero missing’ phenomenon, when energizing the cable connected to the shunt reactors. When the current flowing in an AC system contains a high enough decaying DC component (greater than peak ac current), the current waveform may not cross the zero value for number of cycles as shown in Fig. 3. This phenomenon is called “zero missing”. Within the zero-missing period it is may not be possible to open the circuit breaker (depending on the DC current magnitude) and interrupt the current

successfully [1], [3] as a natural current zero does not happen during this period.

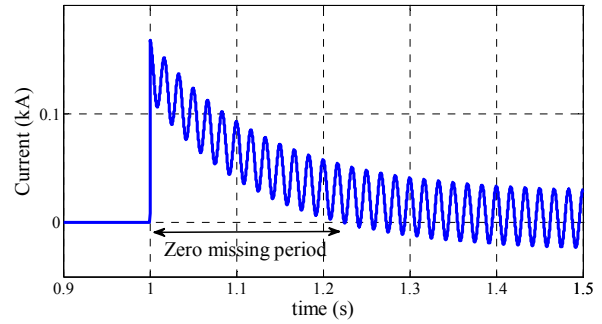


Fig. 3 – Illustration of Zero-missing

A long transmission cable is highly capacitive and the shunt compensation is generally provided at the onshore end of the cable. For the simplicity of explanation, a simple RLC circuit shown in Fig. 4 is used to explain the ‘zero missing’ phenomenon similar to [2].

The circuit shown in Fig. 4 is excited using a sinusoidal voltage and the resulting current across the inductive element should be zero at the switching instant ( $t=0$ ) irrespective of the voltage phase. This inductor current,  $I_L(t)$  has a DC component as well as an AC component. As the AC component lags the voltage by 90 degrees it should be at its negative peak value to maintain the phase lag, if the voltage phase is zero at time  $t=0$ . However, as the resultant current is zero at the switching instant, the inductor current should contain a DC component equal to its AC current magnitude.

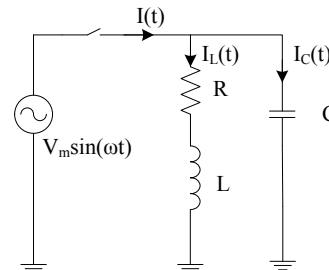


Fig. 4 – Zero-missing phenomenon explanation using a RLC circuit

To further illustrate this,  $I_L(t)$  of Fig. 4 is plotted in Fig. 5. The DC component is clearly visible and decays with time due to the energy loss in the resistor. It can be seen that the inductor current  $I_L(t)$  always contains a zero crossing even with the DC component.

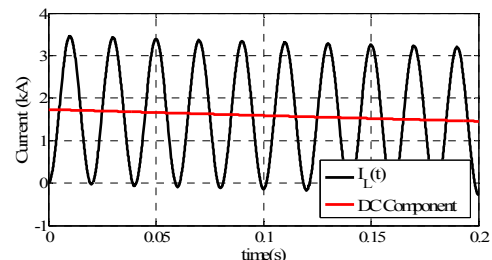


Fig. 5 - Inductor Current for switching at phase angle -  $0^\circ$

The capacitor in parallel also draws a purely sinusoidal current,  $I_C(t)$  and it has approximately a  $180^\circ$  phase shift with the inductor current. This capacitor current cancels out the ac component of the inductor current if the inductive and capacitive reactances are equal in magnitude. This is depicted in Fig. 6 (a), where it can be seen that  $I_C(t)$  and the ac component of  $I_L(t)$  are equal and opposite in phase. Fig. 6 (b) shows the resultant current,  $I(t)$  which is mainly the dc component of the inductor current.

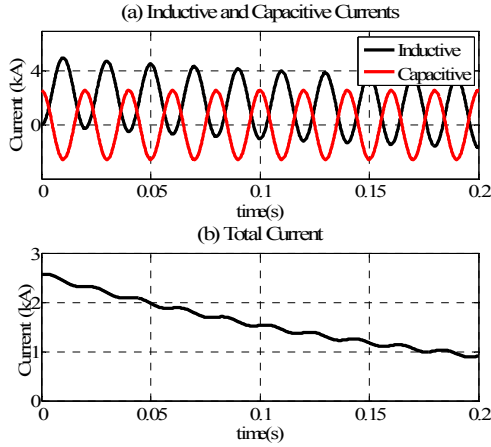


Fig. 6 - Currents of the RLC circuit (for  $\omega L=1/\omega C$ )

Using similar analysis, it can be shown that the ‘zero missing’ phenomenon occurs whenever the inductive reactance is at least half of the capacitive reactance.  $I_L(t)$  and  $I_C(t)$  of this limiting case is shown in Fig. 7 (a). The resultant current,  $I(t)$  is shown in Fig. 7 (b) where the waveform touches the time axis from the beginning of the event.

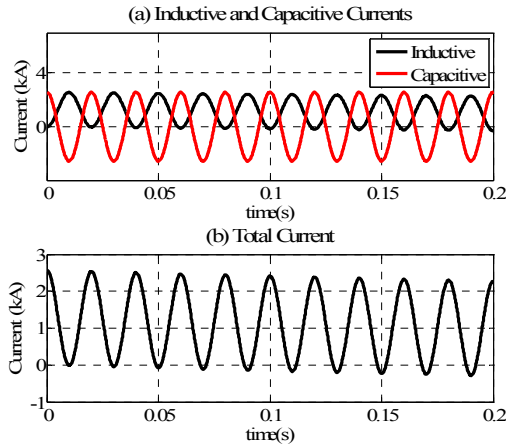


Fig. 7 - Currents of the RLC circuit (for  $\omega L=1/2(1/\omega C)$ )

Therefore, when the inductive current is larger than this limiting case, there is always going to be a zero missing situation.

The circuit shown in Fig. 4 can be solved for currents mathematically as follows;

$$I_L(t) = \frac{V_m}{L^2\omega^2 + R^2} \cdot \left[ L\omega \cdot e^{-\frac{R}{L}t} - L\omega \cdot \cos(\omega t) + R \cdot \sin(\omega t) \right] \quad (1)$$

When  $R \ll L\omega$ ,

$$\frac{1}{L^2\omega^2 + R^2} \approx \frac{1}{L^2\omega^2}, \text{ Therefore,}$$

$$I_L(t) \approx V_m \cdot \left( \frac{1}{L\omega} \cdot e^{-\frac{R}{L}t} - \frac{1}{L\omega} \cdot \cos(\omega t) + \frac{R}{L^2\omega^2} \cdot \sin(\omega t) \right) \quad (2)$$

$$I_C(t) = V_m \cdot C\omega \cos(\omega t) \quad (3)$$

Therefore, when  $C\omega = 1/(L\omega)$ , the total current  $I(t)$  can be found approximately,

$$I(t) \approx V_m \cdot \left( \frac{1}{L\omega} \cdot e^{-\frac{R}{L}t} + \frac{R}{L^2\omega^2} \cdot \sin(\omega t) \right) \quad (4)$$

Here, the magnitude of the sinusoidal component is very small as  $R$  is generally much smaller than  $L\omega$ . This demonstrates that when the capacitive and inductive reactances are equal, current drawn by the circuit is mainly an exponentially decaying DC.

In the Triton Knoll design, the cables supply approximately 330 MVar of capacitive reactive power. The proposed total shunt reactance (fixed) is 270 MVar. Thus, based on the above theoretical discussion, the potential for zero missing is present.

#### IV. SIMULATION RESULTS AND OBSERVATIONS

Phase 1 of the AC transmission system discussed in section II. is modeled in an emt type program (PSCAD/EMTDC) as depicted in Fig. 8. Both onshore and offshore cables are simulated using appropriate frequency dependent models [5] of coaxial and pipe-type cables.

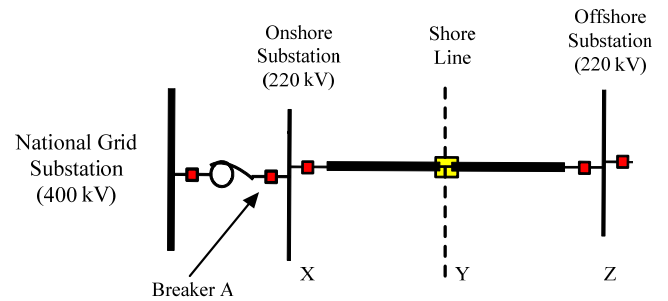


Fig. 8 – Phase 1 of the Ac transmission system including the 400/220 kV transformer

First, the simulations are carried out with all the reactors placed at the on-shore substation end (X) and the currents are observed following the closing of the breaker A (at 1s in the simulation). Phase angle of the voltage at the point of switching was maintained at  $0^\circ$  to identify the worst case of zero missing.

A 330 MVA 400/220 kV transformer bank consisting of 3 single phase two winding units were used in the study model.

The transformer saturation characteristics (flux linkage vs. magnetizing current) assumed for the study are shown in Fig. 9. The saturation characteristics shown in Fig. 9 and the leakage reactance (10 %) between the windings (transformer losses were neglected to simulate a ‘worst case’) are sufficient to represent the transformer in enough detail for this investigation.

In order to highlight the impact of transformer saturation, simulations were carried out assuming a linear core as well. Resulting waveforms are presented in Fig. 10.

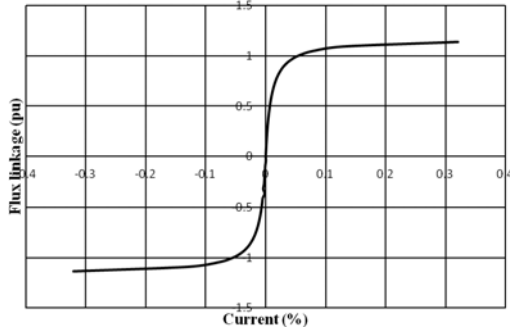


Fig. 9 – Saturation Curve for the transformer

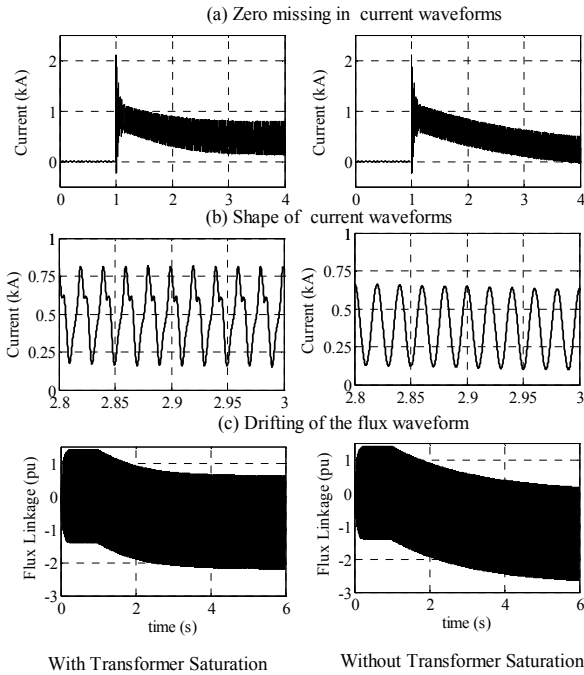


Fig. 10 –Simulation results for the base case

As seen in Fig. 10, transformer saturation has impacted the zero missing time duration and the current waveform is also distorted. This is attributed to the drifting of flux due to the initial offset in the current. Such drifting in flux increases the magnetizing current. Since this observation was not discussed in previous publications, a detailed analysis was carried out to justify the simulation observations.

## V. IMPACT OF THE TRANSFORMER ON ZERO MISSING

The analysis in [1], [2] as well as in the analysis of section III. an ideal voltage source was used to represent the system. However, in practice and in the case of Triton Knoll, a transformer is present between the substation and the cable (Fig. 11). Analysis based on the circuit of Fig. 11 is used to explain the flux drift and the corresponding half cycle saturation of the transformer core.

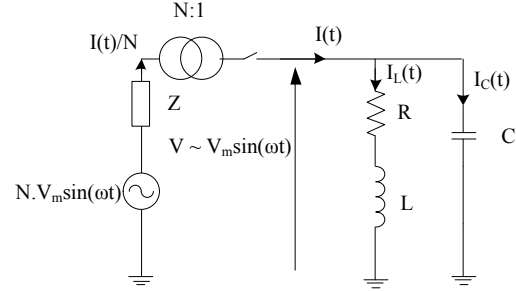


Fig. 11 – Circuit for the flux calculation

If we assume that the transformer secondary side voltage immediately after breaker closing is  $V_m \sin(\omega t)$  (i.e. closed at a voltage zero), sum of (2) and (3) is valid for the circuit current. Therefore,  $I(t)$  can be written as,

$$I(t) = I_L(t) + I_C(t)$$

Substituting from (2) and (3),

$$I(t) = A \cdot e^{-\frac{t}{\tau}} + B \cdot \sin(\omega t + \phi) \quad (5)$$

Where,

$$A = \frac{V_m}{L\omega}, \quad B = V_m \cdot \sqrt{x^2 + y^2}, \quad \tau = \frac{L}{R^*}$$

$$x = \frac{R}{L\omega}, \quad y = \left[ C\omega - \frac{1}{L\omega} \right]$$

Here,  $R^*$  can be taken as  $R$  (in Fig. 11), however, if there is a significant resistive component in the source impedance  $Z$ , it is also taken into account approximately by having,

$$R^* = R + \frac{1}{N^2} \cdot R_Z \quad (6)$$

$R_Z$  is given by,  $Z = R_Z + j\omega L_Z$

Voltage and flux linkage ( $\lambda$ ) at the transformer primary side are related by,

$$\frac{d\lambda}{dt} = N \cdot V_m \sin(\omega t) - R_Z \cdot \frac{1}{N} \cdot I(t) - L_Z \cdot \frac{1}{N} \cdot \frac{dI(t)}{dt} \quad (7)$$

By integrating (7) after substituting  $I(t)$  in (5), it is possible to get an expression for the flux linkage  $\lambda(t)$ . It should be noted that the indefinite integral of the  $N \cdot V_m \sin(\omega t)$  term should be used as we need the steady state value of the flux corresponding to that term. However, rest of the terms should be integrated over an interval  $[0, t]$ . The resulting expression is shown in (8).

$$\lambda(t) = -\frac{N \cdot V_m}{\omega} \cos(\omega t) - \frac{R_z}{N} \left[ A\tau - A\tau \cdot e^{-\frac{t}{\tau}} + \frac{B}{\omega} \cdot \cos(\phi) - \frac{B}{\omega} \cdot \cos(\omega t + \phi) \right] - \frac{L_z}{N} \left[ A \cdot e^{-\frac{t}{\tau}} - B \cdot \sin(\omega t + \phi) \right] \quad (8)$$

The behavior suggested by the analytical equation (8) is consistent with the observed simulation results (Section VI. ).

## VI. RESULTS

The simulation results presented in this section are for the case where the total reactance of 270 MVAR is at the onshore substation (point X in Fig. 8). Breaker A is closed at 1s. ‘Zero missing’ phenomenon is observed as shown in Fig. 12 and the zero missing time duration is approximately 2.67s.

Using the transformer model available in PSCAD/EMTDC, the flux linkage waveforms are obtained and they are compared with the flux waveforms predicted by the analytical expression (8). The close agreement of the flux waveforms shown in Fig. 13 (b) is a validation of simulation results and observations.

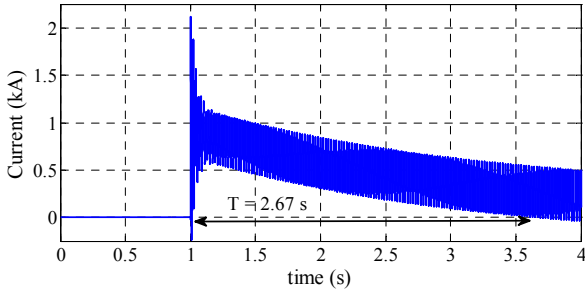


Fig. 12 – Current waveform (Onshore - 270MVAR)

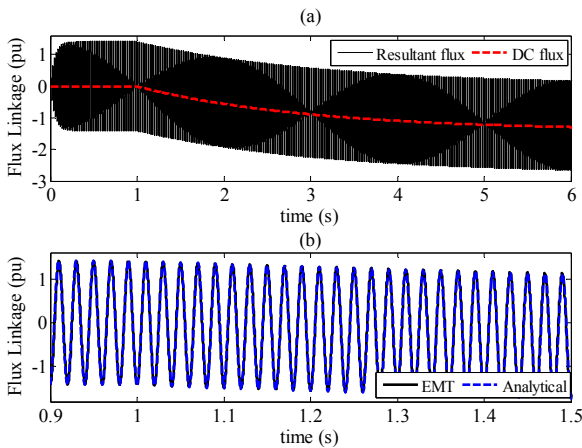


Fig. 13 – Flux linkage comparison

## VII. MITIGATION OPTIONS

‘Zero missing’ phenomenon is identified as one of the main concerns to be addressed and the following mitigation options are investigated.

- A. Distribution of the total shunt reactance over different location on the cable.
- B. Use of breaker pre insertion resistors

Additionally, a special purpose circuit breaker capable of point-on-wave switching operations can be employed to minimize the effects of ‘zero missing’ phenomenon. However, this possibility was not considered in this study.

### A. Distribution of shunt reactance over different locations on the cable

Under this investigation, different reactor values are placed at X, Y and Z points of Fig. 8 and the zero missing time durations are observed. The total shunt compensation is kept constant at 270 MVAR. A summary of the scenarios considered and the ‘zero missing’ durations are given in TABLE 1.

TABLE 1  
ZERO MISSING TIMES FOR DIFFERENT SHUNT REACTOR POSITIONING

Configuration s	Shunt Compensation (MVAR)			Zero missing Period (s)
	X	Y	Z	
1	270	-	-	2.67
2	120	150	-	1.97
3	90	90	90	1.47
4	-	-	270	0.24

Configuration 4 has the shortest zero missing duration. This is due to the fact that the cable resistances of both cables contribute to damp the dc component of the current. Fig. 14 shows the corresponding current waveform.

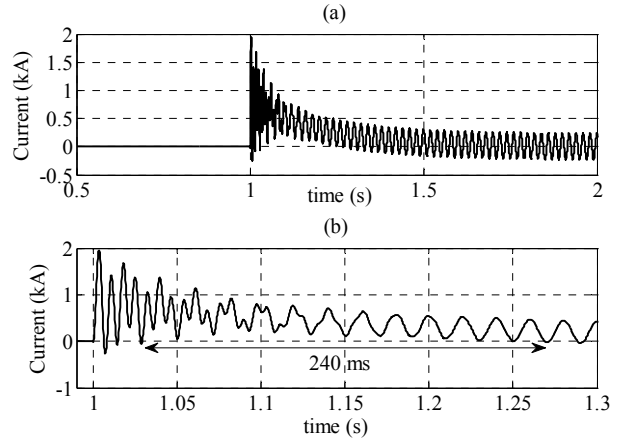


Fig. 14 – Current waveform when all reactors placed at offshore end (a. current waveform, b. zoomed view)

While configuration 4 maybe viable, it is not the optimal solution from the cost as well as the practical implementation point of view. Installing additional equipment on the offshore platform adds to the overall weight on the platform and hence cost and operational issues. Thus, the option of having a breaker pre insertion resistance along with configuration 2 is considered the most viable solution.

### B. Inclusion of breaker pre-insertion resistance

According to the approximate method provided in [1] for the pre insertion resistance calculation, a 114  $\Omega$  resistance is required to obtain a zero crossing after 10ms of breaker closure for the Triton Knoll design (all 270 MVAR connected at point X). As shown in Fig. 15, simulation results also agree with this calculation.

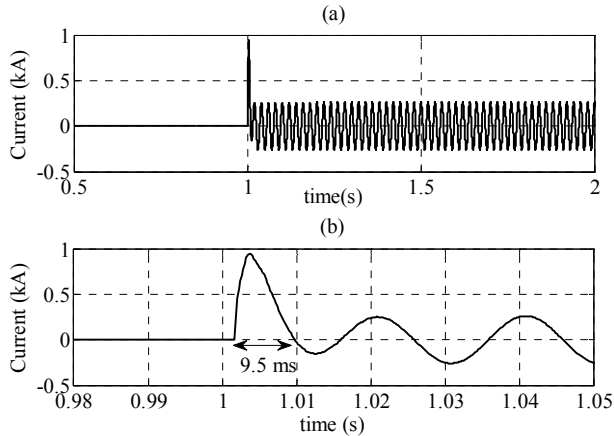


Fig. 15 – Current waveform with pre-insertion resistance of 114  $\Omega$  (a. current waveform, b. zoomed view)

Simulation results indicate that a pre insertion resistance greater than 10 Ohms will reduce the zero miss duration to be less than 5 cycles. Simulation results with a 10 Ohm pre insertion resistor is shown in Fig. 16.

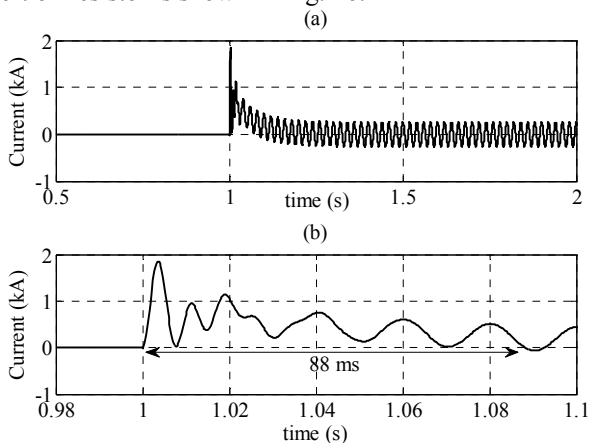


Fig. 16 – Current waveform with pre-insertion resistance of 10  $\Omega$

## VIII. CONCLUSIONS

Transients following the energization of AC transmission system interconnecting Triton Knoll wind power plant and the Bicker Fen substation are investigated and the ‘zero missing’ phenomenon is identified as a major concern to be addressed. Initial simulations showed that the ‘zero missing’ phenomenon is associated with distorted current waveforms due to transformer saturation. This observation is analyzed in detail and is considered a contribution of this paper. Analytical derivations were compared with detailed simulations to verify simulation observations.

Mitigation methods capable of reducing the zero miss time

duration are discussed. The mitigation methods investigated include the distribution of the total shunt reactance over different locations of the cable and the use of breaker pre insertion resistor.

## IX. REFERENCES

- [1] F. F. Da Silva, C. L. Bak, U. S. Gudmundsdottir, W. Wiechowski, and M. R. Knardrupgård, "Methods to minimize zero-missing phenomenon," *IEEE Trans. Power Delivery*, vol. 25, pp. 2923-2930, Oct. 2010.
- [2] F. F. Da Silva, C. L. Bak, U. S. Gudmundsdottir, W. Wiechowski, and M. R. Knardrupgård, "Use of a Pre-Insertion Resistor to Minimize Zero-Missing Phenomenon and Switching Overvoltages," in *Proc. 2009 IEEE Power Engineering Society General Meeting*, pp. 1-7.
- [3] "Connecticut cable transient and harmonics study for phase 2: Final rep." GE Power Systems Energy Consulting, 2003.
- [4] RWE Triton Knoll newsletter, Sept. 2012
- [5] A. Morched, B. Gustavsen, M. Tartibi, "A universal model for accurate calculation of electromagnetic transients on overhead lines and underground cables", *IEEE Transactions on Power Delivery*, vol.14, no.3, pp.1032-1038, Jul 1999.